



ELSEVIER

SCIENCE @ DIRECT®

PHYSICS LETTERS B

Physics Letters B 555 (2003) 71–82

www.elsevier.com/locate/npe

Improved determination of the electroweak penguin contribution to ϵ'/ϵ in the chiral limit

Vincenzo Cirigliano^a, John F. Donoghue^b, Eugene Golowich^b, Kim Maltman^{c,d}

^a *Departament de Física Teòrica, IFIC, Universitat de València, CSIC, Apt. Correus 2085, E-46071 València, Spain*

^b *Physics Department, University of Massachusetts, Amherst, MA 01003, USA*

^c *Department of Mathematics and Statistics, York University, 4700 Keele St., Toronto ON M3J 1P3, Canada*

^d *CSSM, University of Adelaide, Adelaide, SA 5005, Australia*

Received 3 December 2002; accepted 5 January 2003

Editor: H. Georgi

Abstract

We perform a finite energy sum rule analysis of the flavor ud two-point V – A current correlator, $\Delta\Pi(Q^2)$. The analysis, which is performed using both the ALEPH and OPAL databases for the V – A spectral function, $\Delta\rho$, allows us to extract the dimension six V – A OPE coefficient, a_6 , which is related to the matrix element of the electroweak penguin operator, \mathcal{Q}_8 , by chiral symmetry. The result for a_6 leads directly to the improved (chiral limit) determination $\epsilon'/\epsilon = (-15.0 \pm 2.7) \times 10^{-4}$. Determination of higher dimension OPE contributions also allows us to perform an independent test using a low-scale constrained dispersive analysis, which provides a highly nontrivial consistency check of the results.

© 2003 Elsevier Science B.V. Open access under [CC BY license](http://creativecommons.org/licenses/by/3.0/).

1. Introduction

Intense effort carried out over many years to measure ϵ'/ϵ has yielded the precise determination [1]

$$[\epsilon'/\epsilon]_{\text{EXPT}} = (16.6 \pm 1.6) \times 10^{-4}. \quad (1)$$

In the Standard Model, the primary dependence of ϵ'/ϵ lies with the K -to- 2π matrix elements of the QCD penguin (\mathcal{Q}_6) and EW penguin (\mathcal{Q}_8) operators [2]. For example, in the $\overline{\text{MS}}$ -NDR scheme at scale

$\mu = 2 \text{ GeV}$ one has [3]

$$\begin{aligned} \frac{\epsilon'}{\epsilon} = & 20 \times 10^{-4} \left(\frac{\text{Im } \lambda_t}{1.3 \times 10^{-3}} \right) \\ & \times \left[-2.0 \text{ GeV}^{-3} \langle (\pi\pi)_{I=0} | \mathcal{Q}_6 | K^0 \rangle_{2 \text{ GeV}} \right. \\ & \times (1 - \Omega_{\text{IB}}) \\ & - 0.50 \text{ GeV}^{-3} \langle (\pi\pi)_{I=2} | \mathcal{Q}_8 | K^0 \rangle_{2 \text{ GeV}} \\ & \left. - 0.06 \right], \quad (2) \end{aligned}$$

where the factor Ω_{IB} accounts for effects of isospin breaking. The electroweak penguin (EWP) operator, the subject of our attention in this Letter, is given by

$$\mathcal{Q}_8 \equiv \bar{s}_a \Gamma_L^\mu d_b \left(\bar{u}_b \Gamma_\mu^R u_a - \frac{1}{2} \bar{d}_b \Gamma_\mu^R d_a - \frac{1}{2} \bar{s}_b \Gamma_\mu^R s_a \right), \quad (3)$$

E-mail addresses: vincenzo.cirigliano@ific.uv.es

(V. Cirigliano), donoghue@physics.umass.edu (J.F. Donoghue),

golowich@physics.umass.edu (E. Golowich),

kmaltman@physics.adelaide.edu.au (K. Maltman).

where $\Gamma_{L,R}^\mu \equiv \gamma^\mu (1 \pm \gamma_5)$ and a, b are color indices.

In a previous paper [4], we worked in the SU(3) chiral limit ($m_u = m_d = m_s = 0$) and obtained for the EWP contribution to ϵ'/ϵ ,

$$[\epsilon'/\epsilon]_{\text{EWP}} = (-22 \pm 7) \times 10^{-4}. \quad (4)$$

The 32% uncertainty in this determination is small enough to allow the conclusion that the chiral value for $[\epsilon'/\epsilon]_{\text{EWP}}$ is negative and rather large (roughly the magnitude of the experimental signal for ϵ'/ϵ). Moreover, we understand the source of the uncertainty. Chiral sum rules used in Ref. [4] to obtain the result in Eq. (4) require knowledge of V–A spectral functions over *all* energy. However, data¹ provides input only up to the scale $s = m_\tau^2$. We overcame this problem in Ref. [4] by employing the chiral sum rules of Weinberg [5] and others [6] as constraints. In all, our procedure was subject to errors coming from the spectral function data set [7,8] as well as those associated with quantities (the pion decay constant and the pion electromagnetic mass splitting) whose values must be estimated in the chiral limit [9].

It is our purpose in this Letter to report on an improved chiral determination of $[\epsilon'/\epsilon]_{\text{EWP}}$ (i.e., one with reduced uncertainty) which uses finite energy sum rules (FESR) as the main theoretical technique [10]. However, it is necessary to summarize briefly aspects of Ref. [4] since this new approach relies upon a number of details derived there. We do this in Section 2, then go on to describe the FESR analysis in Section 3, discuss the implications for the electroweak matrix elements in Section 4, and summarize our findings in Section 5. A more detailed discussion of the FESR analysis is presented in a companion paper [11].

2. Chiral properties of $\langle (\pi\pi)_{I=2} | \mathcal{Q}_{7,8} | K^0 \rangle$

In the chiral limit the matrix elements $\langle (\pi\pi)_{I=2} | \mathcal{Q}_8 | K^0 \rangle_\mu$ and also $\langle (\pi\pi)_{I=2} | \mathcal{Q}_7 | K^0 \rangle_\mu$ become expressible in terms of vacuum matrix elements $\langle \mathcal{O}_1 \rangle_\mu$

¹ In this Letter we work with the ALEPH and OPAL spectral functions displayed in Fig. 1(a), (b). This normalization for $\Delta\rho$ corresponds to the flavor ud two-point V–A current correlator and has *twice* the magnitude employed in Ref. [4].

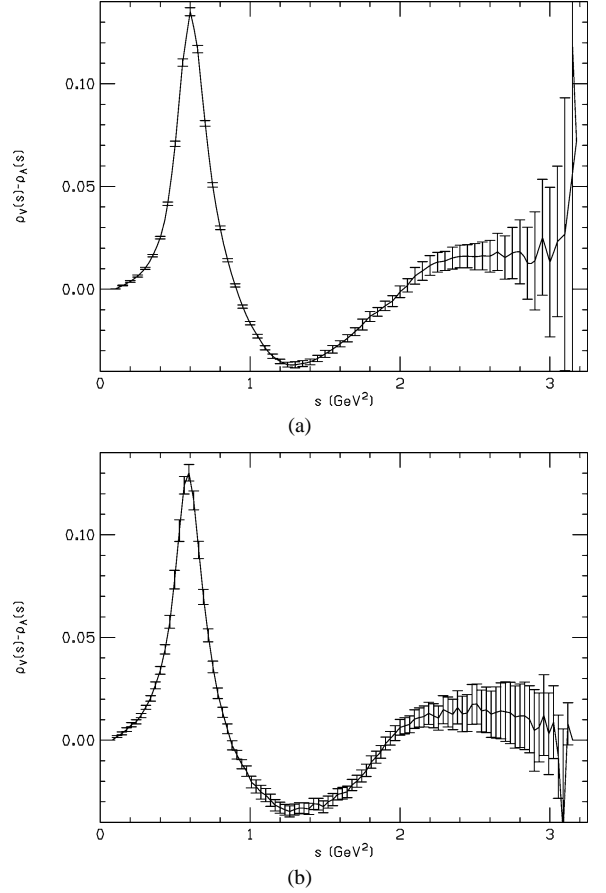


Fig. 1. (a) ALEPH data; (b) OPAL data.

and $\langle \mathcal{O}_8 \rangle_\mu$, [4,12]

$$\begin{aligned} \lim_{p=0} \langle (\pi\pi)_{I=2} | \mathcal{Q}_7 | K^0 \rangle_\mu &= -\frac{2}{F_\pi^{(0)3}} \langle \mathcal{O}_1 \rangle_\mu, \\ \lim_{p=0} \langle (\pi\pi)_{I=2} | \mathcal{Q}_8 | K^0 \rangle_\mu &= -\frac{2}{F_\pi^{(0)3}} \left[\frac{1}{3} \langle \mathcal{O}_1 \rangle_\mu + \frac{1}{2} \langle \mathcal{O}_8 \rangle_\mu \right], \end{aligned} \quad (5)$$

where $F_\pi^{(0)}$ is the pion decay constant evaluated in the chiral limit.² The sum rule analysis of Ref. [4]

² The operators $\mathcal{O}_{1,8}$ are defined as

$$\begin{aligned} \mathcal{O}_1 &\equiv \bar{q}\gamma_\mu \frac{\tau_3}{2} q \bar{q}\gamma^\mu \frac{\tau_3}{2} q - \bar{q}\gamma_\mu \gamma_5 \frac{\tau_3}{2} q \bar{q}\gamma^\mu \gamma_5 \frac{\tau_3}{2} q, \\ \mathcal{O}_8 &\equiv \bar{q}\gamma_\mu \lambda^a \frac{\tau_3}{2} q \bar{q}\gamma^\mu \lambda^a \frac{\tau_3}{2} q - \bar{q}\gamma_\mu \gamma_5 \lambda^a \frac{\tau_3}{2} q \bar{q}\gamma^\mu \gamma_5 \lambda^a \frac{\tau_3}{2} q. \end{aligned}$$

implies that the numerical effect of $\langle \mathcal{O}_1 \rangle_{2 \text{ GeV}}$ on $\lim_{p=0} \langle (\pi\pi)_{I=2} | \mathcal{Q}_8 | K^0 \rangle_{2 \text{ GeV}}$ is just 2.5% that of $\langle \mathcal{O}_8 \rangle_{2 \text{ GeV}}$. This means that at the level of accuracy we can realistically hope to achieve for $\lim_{p=0} \langle (\pi\pi)_{I=2} | \mathcal{Q}_8 | K^0 \rangle_{2 \text{ GeV}}$, it is sufficient to ignore the contribution from $\langle \mathcal{O}_1 \rangle_{2 \text{ GeV}}$ and focus on just the quantity $\langle \mathcal{O}_8 \rangle_{2 \text{ GeV}}$. We return to this point at the end of this section.

2.1. Getting $\langle \mathcal{O}_8 \rangle_\mu$ from the OPE of $\Delta\Pi$

Much about $\langle \mathcal{O}_8 \rangle_\mu$ (and also about $\langle \mathcal{O}_1 \rangle_\mu$) can be learned from the flavor ud V–A correlator. Defining $\Delta\Pi \equiv \Pi_V^{(0+1)} - \Pi_A^{(0+1)}$, where the superscript (0+1) indicates the sum of the spin 0 and 1 parts of the relevant correlator, the dispersive representation of $\Delta\Pi$ is

$$\Delta\Pi(Q^2) = -\frac{2F_\pi^2}{m_\pi^2 + Q^2} + \int_{s_{\text{thr}}}^{\infty} ds \frac{\Delta\rho(s)}{s + Q^2}. \quad (6)$$

Here, $Q^2 \equiv -q^2$ is the variable for space-like momenta and $\Delta\rho \equiv \rho_V^{(0+1)} - \rho_A^{(0+1)}$ is the spectral function of $\Delta\Pi$. For large space-like momenta $Q^2 \gg \Lambda_{\text{QCD}}^2$ and through $\mathcal{O}(\alpha_s^2)$ in QCD counting, $\Delta\Pi(Q^2)$ can be represented via the operator product expansion (OPE)

$$\Delta\Pi(Q^2) \sim \sum_d \frac{1}{Q^d} \left[a_d(\mu) + b_d(\mu) \ln \frac{Q^2}{\mu^2} \right] \quad (d = 2, 4, 6, 8, 10, \dots), \quad (7)$$

where $a_d(\mu)$ and $b_d(\mu)$ are combinations of vacuum expectation values of local operators of dimension d . In the chiral limit, the contributions from dimensions $d = 2, 4$ are absent and the above sum begins with dimension $d = 6$.

The $d = 6$ OPE coefficients a_6, b_6 are of special interest because they are related to the vacuum matrix elements $\langle \mathcal{O}_8 \rangle_\mu$ and $\langle \mathcal{O}_1 \rangle_\mu$. Since the relations are renormalization scheme dependent we consider for definiteness $\overline{\text{MS}}$ renormalization with NDR and HV prescriptions for γ_5 and the evanescent operator basis used in Refs. [13,14]. Including $\mathcal{O}(\alpha_s^2)$ terms this leads

to

$$\begin{aligned} a_6(\mu) &= 2[2\pi \langle \alpha_s \mathcal{O}_8 \rangle_\mu + A_8 \langle \alpha_s^2 \mathcal{O}_8 \rangle_\mu + A_1 \langle \alpha_s^2 \mathcal{O}_1 \rangle_\mu], \\ b_6(\mu) &= 2[B_8 \langle \alpha_s^2 \mathcal{O}_8 \rangle_\mu + B_1 \langle \alpha_s^2 \mathcal{O}_1 \rangle_\mu]. \end{aligned} \quad (8)$$

In terms of their dependence on the NDR or HV renormalization scheme, the coefficients A_1, A_8 and B_1, B_8 are given by

	NDR	HV
A_1	2	-10/3
A_8	205/36	169/36
B_1	8/3	8/3
B_8	-2/3	-2/3

where we work with three colors ($N_c = 3$) and four active flavors ($n_f = 4$).

Given our earlier discussion following Eq. (5) about the dominance of $\langle \mathcal{O}_8 \rangle_{2 \text{ GeV}}$ relative to $\langle \mathcal{O}_1 \rangle_{2 \text{ GeV}}$, it follows from Eq. (8) that an attractive alternative to the sum rule procedure of Ref. [4] for finding $\lim_{p=0} \langle (\pi\pi)_{I=2} | \mathcal{Q}_8 | K^0 \rangle_\mu$ is to determine the OPE coefficient $a_6(\mu)$. The FESR approach is naturally structured to do just that. Moreover, since only knowledge of $\Delta\rho$ in the data region is required, the prospect of an improved determination is well motivated.

2.2. The sum rule approach revisited

Independently from the method described in the preceding section, knowledge gained from the FESR analysis of the higher-dimensional OPE coefficients $\{a_{d \geq 8}\}$ allows us to return to the sum rule method of Ref. [4] and perform an improved determination of $\langle \mathcal{O}_8 \rangle_\mu$ and $\langle \mathcal{O}_1 \rangle_\mu$. This hybrid method provides a nontrivial consistency check on the FESR results of this Letter. We summarize this approach in the following.

The two sum rules derived in Ref. [4] are

$$\begin{aligned} \langle \mathcal{O}_1 \rangle_\mu - \frac{3C_8}{8\pi} \langle \alpha_s \mathcal{O}_8 \rangle_\mu &= \frac{3}{(4\pi)^2} [I_1(\mu) + H_1(\mu)], \\ 2\pi \langle \alpha_s \mathcal{O}_8 \rangle_\mu + A_1 \langle \alpha_s^2 \mathcal{O}_1 \rangle_\mu + A_8 \langle \alpha_s^2 \mathcal{O}_8 \rangle_\mu &= I_8(\mu) - H_8(\mu), \end{aligned} \quad (10)$$

In the above, $q = u, d, s$, τ_3 is a Pauli (flavor) matrix, $\{\lambda^a\}$ are the Gell-Mann color matrices and the subscripts on $\mathcal{O}_1, \mathcal{O}_8$ refer to the color carried by their currents.

where

$$I_1 = \frac{1}{2} \int_0^\infty ds s^2 \ln\left(\frac{s + \mu^2}{s}\right) \Delta\rho(s),$$

$$I_8 = \frac{1}{2} \int_0^\infty ds s^2 \frac{\mu^2}{s + \mu^2} \Delta\rho(s) \quad (11)$$

and

$$H_1 = \frac{1}{2} \sum_{d \geq 8} \frac{2}{d-6} \frac{a_d(\mu)}{\mu^{d-6}}, \quad H_8 = \frac{1}{2} \sum_{d \geq 8} \frac{a_d(\mu)}{\mu^{d-6}}. \quad (12)$$

The above definitions of $I_{1,8}$ and $H_{1,8}$ coincide with the ones given in Ref. [4]—the prefactors of $1/2$ simply account for the different normalization of $\Delta\rho$ used in this work. The scheme dependent quantities A_1, A_8 of Eq. (10) are given in Eq. (9) and C_8 appears in Table 1 of Ref. [4]. Observe that even if the higher dimension OPE coefficients in $H_{1,8}$ are not known, the sum rules can nonetheless be successfully evaluated. One simply chooses a sufficiently large scale μ , e.g., at $\mu = 4$ GeV, to suppress contributions from the $\{a_{d \geq 8}\}$ and then uses the renormalization group equations to evolve down to the scale $\mu = 2$ GeV. This was the procedure adopted in Ref. [4]. However, it turns out that the uncertainty in evaluating the spectral integrals in Eq. (10) grows with increasing μ and this source of error is ultimately communicated to the sum rule prediction for $\langle(\pi\pi)_{I=2} | Q_{7,8} | K^0 \rangle_{\mu=2}^{\overline{\text{MS}}}$. Our FESR determination of the $\{a_{d \geq 8}\}$ allows us to avoid this difficulty by allowing evaluation of the sum rules directly at $\mu = 2$ GeV and thus leads to reduced uncertainties in the matrix element values. Results of this hybrid approach are presented in Section 4.

We now turn to a discussion of our FESR analysis.

3. FESR analysis

We begin with the following exact consequence of Cauchy's theorem (plus the rigorous statement of analytic structure for $\Delta\Pi$),

$$\int_{s_{\text{th}}}^{s_0} ds w(s) \Delta\rho(s) - 2F_\pi^2 w(m_\pi^2)$$

$$= -\frac{1}{2\pi i} \oint_{|s|=s_0} ds w(s) \Delta\Pi(s), \quad (13)$$

where the contour of integration for $\Delta\Pi$ is a circle of radius s_0 (cf. Fig. 2) and $w(s)$ is analytic on and within the given contour. The additive term proportional to F_π^2 on the left-hand side of Eq. (13) arises from the pion pole. The object of FESRs is to replace $\Delta\Pi$ on the circle by the asymptotic OPE form $\Delta\Pi_{\text{OPE}}$ (see Eq. (7)) and thereby obtain constraints on the OPE coefficients in terms of data from knowledge of the spectral function $\Delta\rho$.

Implementing this procedure but making no additional assumptions, we can then write compactly

$$\int_{s_{\text{th}}}^{s_0} ds w(s) \Delta\rho(s) - 2F_\pi^2 w(m_\pi^2)$$

$$= -\frac{1}{2\pi i} \oint_{|s|=s_0} ds w(s) \Delta\Pi_{\text{OPE}}(s) - R[s_0, w], \quad (14)$$

where the quantity $R[s_0, w]$ is defined as

$$R[s_0, w] \equiv -\frac{1}{2\pi i} \oint_{|s|=s_0} ds w(s) [\Delta\Pi_{\text{OPE}}(s) - \Delta\Pi(s)]. \quad (15)$$

While Eqs. (14), (15) are valid for any weight $w(s)$ analytic in a region including the contour of Fig. 2, the presence of the a priori unknown additive term $R[s_0, w]$ generates a systematic uncertainty in the extraction of the OPE coefficients a_d via Eq. (14). Therefore it is highly desirable to work with a range

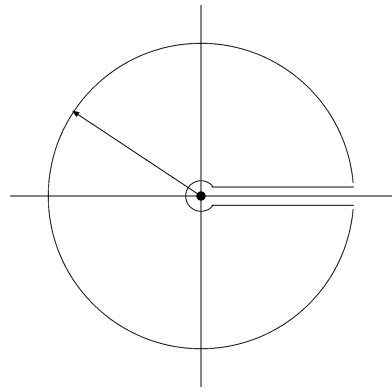


Fig. 2. FESR contour.

of s_0 values and with weight functions $w(s)$ such that the remainder term $R[s_0, w]$ is small compared to the spectral integral itself. To accomplish this, we rely on the observation that for $|s|$ large enough ($s_0 \gg \Lambda_{\text{QCD}}^2$), the OPE provides a good representation of the full correlator along the whole circle except in a region localized around the time-like axis. The physics of this breakdown is given by the arguments of Poggio, Quinn and Weinberg [15]. As a consequence one expects that weights with a zero at $s = s_0$, de-emphasizing the region where the OPE fails, are good candidates to generate a small-sized $R[s_0, w]$ even for the relatively low s_0 values, between 2 GeV^2 and m_τ^2 , as used in our FESR analysis. Arguments which justify the choice of this range are given in Section 3.2 following Eq. (21).

Supporting evidence for the procedure outlined above is provided by one of us in previous studies of the V and A correlators [10,16]. Internal consistency checks of the V–A analysis are also possible (see Section 3.2 for a further discussion of this point). Moreover, a study of models with pole contributions which violate duality shows that the method succeeds in extracting the asymptotic values of the corresponding a_d coefficients, even in the presence of such duality violation [11].

3.1. Choice of FESR weights

To complete preparations for performing our FESR study, the highly nontrivial procedure of constructing appropriate weights $w(s)$ must be addressed. Three basic considerations govern our choice of weights:

- (1) Because the OPE is known to fail along the $\text{Re } s \geq 0$ axis [15], we employ only ‘pinched’ weights $w(s_0) = 0$. In particular, recall that the kinematic weight ($w(y_\tau) = (1 - y_\tau)^2(1 + 2y_\tau)$ with $y_\tau \equiv s/m_\tau^2$), which must be unfolded from the experimental decay distribution in order to obtain $\Delta\rho$, contains a double zero at $s = m_\tau^2$. To avoid enhancements of contributions from the endpoint region, where experimental errors are large, we therefore employ weights $w(y) = (1 - y)^2 p(y)$ ($y \equiv s/s_0$ and $p(y)$ is a polynomial) which also have a double zero at $s = s_0$. An earlier study [16] has demonstrated that the suppression thus produced suffices to circumvent the OPE breakdown.
- (2) In order to maximize the statistical signal, the weights should be such that large cancellations in the difference between the separate V and A spectral integrals are avoided.
- (3) The separation of contributions with different dimension in a given pinch-weighted FESR (pFESR) relies on the fact that the integrated OPE contributions with different d scale differently with s_0 . When one works in a limited window of s_0 values, the accuracy with which one can perform this separation decreases as the number of contributing a_d terms increases. We, therefore, work with weights such that the minimum number (two) of a_d contributions occurs in any of our sum rules.

The above points are elaborated upon in Ref. [11].

The FESR equations for a set of weights, $\{w_n\}$, are of the general form

$$J_n(s_0) = f_n(a_d, a_{d'}, b_d, b_{d'}; s_0). \quad (16)$$

The quantity $J_n(s_0)$ is defined as

$$J_n(s_0) \equiv \int_0^{s_0} ds w_n(y) \Delta\rho(s) - 2F_\pi^2 w_n(m_\pi^2) - c_n^{(4)}, \quad (17)$$

where $y \equiv s/s_0$ and $c_n^{(4)}$ is the contribution from the dimension-four part of the OPE.³

The functions f_n represent the OPE terms with $d \geq 6$ integrated on the $|s| = s_0$ circle. Polynomial weights of increasing degree allow one to extract condensates a_d of increasing dimension. We use as starting point for our analysis the sum rules based on the weights of the lowest degree satisfying the above criteria. We have also explored generalizations to higher degree polynomials, and report details of this analysis elsewhere [11].

The lowest degree weights satisfying our criteria turn out to have degree three. The one which produces the smallest relative errors on the spectral integrals is

$$w_1(y) = (1 - y)^2(1 - 3y). \quad (18)$$

³ All the $c_n^{(4)}$ terms ($n = 1, 2$) are known explicitly up to $O(\alpha_s^2)$ and are numerically small, being proportional to the pion mass [11]. The $2F_\pi^2 w_n(m_\pi^2)$ terms are likewise small in our analysis, except for the case of the weight w_1 , given in Eq. (18).

An independent choice, also giving small relative errors, is

$$w_2(y) = (1 - y)^2 y. \quad (19)$$

These weights produce OPE integrals involving a_6 and a_8 :

$$\begin{aligned} f_1(a_6, a_8; s_0) &\equiv \frac{7}{s_0^2} a_6 \left[1 + r_6 \log\left(\frac{s_0}{\mu^2}\right) + \frac{3}{14} r_6 \right] + 3 \frac{a_8}{s_0^3}, \\ f_2(a_6, a_8; s_0) &\equiv -\frac{2}{s_0^2} a_6 \left[1 + r_6 \log\left(\frac{s_0}{\mu^2}\right) \right] - \frac{a_8}{s_0^3}. \end{aligned} \quad (20)$$

In Eq. (20) $r_6 \equiv b_6/a_6$, and we neglect all the other $\{b_n\}$ OPE coefficients since they are QCD suppressed ($b_n \sim a_n \alpha_s/\pi$), and are accompanied by small numerical coefficients in the FESR relations. For the ratio r_6 we rely on the explicit NLO QCD expressions of Eq. (8) and on the numerical estimates of $\langle \mathcal{O}_1 \rangle$ and $\langle \mathcal{O}_8 \rangle$ given in Ref. [4].

3.2. FESR analysis: fit and results

The FESR relations of Eqs. (16), (17), (20) for the cases $n = 1, 2$ allow us to impose constraints on the coefficients a_6 and a_8 , as we know $J_{1,2}(s_0)$ from data for $s_0 \leq m_\tau^2$. The treatment of Eq. (17) requires some care due to the presence of strongly correlated errors in the experimental spectral function $\Delta\rho$. Using the covariance matrix for the spectral function data, we calculate the covariance matrix for the set of spectral integrals $J_n(s_0)$: $\text{Cov}(J_n(s_0), J_m(s_0')) \equiv \mathbf{V}_{s_0, s_0'}^{(n, m)}$. Thus we form the weighted least-square function

$$\begin{aligned} \chi^2 = \sum_{s_0} \sum_{n=1,2} (J_n(s_0) - f_n(s_0)) &[\mathbf{V}_{s_0, s_0}^{(n, n)}]^{-1} \\ &\times (J_n(s_0) - f_n(s_0)), \end{aligned} \quad (21)$$

which sums over the set of s_0 values and the two FESR relations ($n = 1, 2$).

We determine the ‘window’ of s_0 values used in our analysis as follows, considering for definiteness the ALEPH data sample. The largest s_0 value (upper edge of the window) is taken as $s_0 = 3.15 \text{ GeV}^2 \simeq m_\tau^2$ simply because it is there that the ALEPH data sample for $\Delta\rho$ runs out. The smallest s_0 value, taken as $s_0 = 1.95 \text{ GeV}^2$, is established by trying ever lower

s_0 values until the extracted $a_6(s_0)$ (which is the most accurately determined OPE coefficient) ceases to be consistent with the previous values obtained from smaller analysis windows. In the final analysis seven equally-spaced values, from $s_0 = 1.95$ to $s_0 = 3.15$ in the ALEPH case, were adopted [11]. We use the ‘diagonal’ least-square function as defined in Eq. (21) to avoid known problems of fits to strongly correlated data [17]. Minimization of χ^2 with respect to variations in a_6 and a_8 yields best fit values for these quantities. With this procedure, as is well known, the one-sigma errors and rms errors do not coincide. The former are smaller, and underestimate the variation of the fitted a_d produced by fluctuations in the input experimental data. All the errors quoted below are the rms errors, i.e., the square roots of the diagonal elements of the covariance matrix for the a_6, a_8 solution set. We thereby arrive at the following results with *renormalization scale set at $\mu = 2 \text{ GeV}$* .

3.2.1. Fit to ALEPH data

$$\begin{aligned} a_6 &= (-44.5 \pm 6.3 \pm 3.4) \times 10^{-4} \text{ GeV}^6, \\ a_8 &= (-61.6 \pm 28.9 \pm 13.8) \times 10^{-4} \text{ GeV}^8. \end{aligned} \quad (22)$$

The first error is associated with the ALEPH covariance matrix. The second is obtained by adding in quadrature uncertainties from parameters which enter the ALEPH normalization of the spectral function and from parameters occurring on the ‘theoretical’ side of the FESR. The correlation coefficient for the fitted parameters is found to be $c(a_6, a_8) = -0.995$, so the output is highly correlated.

By extending the set of weights employed in our analysis, it is possible to construct sum rules which receive contributions from the a_d with $d > 8$.⁴ In this manner we have successfully determined the a_d up to $d = 16$ and thus have evaluated the quantities H_1 and H_8 defined earlier in Eq. (12). We find at the renormalization scale $\mu = 2 \text{ GeV}$,

$$\begin{aligned} H_1 &= (-2.7 \pm 3.6 \pm 0.5) \times 10^{-4} \text{ GeV}^6, \\ H_8 &= (-1.3 \pm 3.0 \pm 2.0) \times 10^{-4} \text{ GeV}^6. \end{aligned} \quad (23)$$

⁴ The process of choosing weights in such a way as to optimize the determination of the higher dimension condensate combinations, a_d , is discussed in more detail in Ref. [11].

Table 1
Summary of FESR results

	a_6 (GeV ⁶)	a_8 (GeV ⁸)
ALEPH	$(-44.5 \pm 7.2) \times 10^{-4}$	$(-61.6 \pm 32.0) \times 10^{-4}$
OPAL	$(-54.3 \pm 7.8) \times 10^{-4}$	$(-13.5 \pm 35.3) \times 10^{-4}$

The first error in $H_{1,8}$ comes from the correlated uncertainties in the OPE coefficients $\{a_d\}$. The second represents our estimate of the error incurred in truncating the OPE sum at $d = 16$. We have obtained this estimate by extending our extraction out to $d = 24$. Although the sums for $H_{1,8}(2 \text{ GeV})$ are found to be well converged by $d = 24$, the extractions of the a_d with $d = 18 \rightarrow 24$ are, however, less certain. We therefore use the difference of the $d = 16$ and $d = 24$ sums as a means of estimating the error associated with employing only the better-determined $d \leq 16$ terms [11].

3.2.2. Fit to OPAL data

$$\begin{aligned} a_6 &= (-54.3 \pm 7.2 \pm 3.1) \times 10^{-4} \text{ GeV}^6, \\ a_8 &= (-13.5 \pm 33.3 \pm 11.7) \times 10^{-4} \text{ GeV}^8. \end{aligned} \quad (24)$$

The first error is associated with the OPAL covariance matrix, and the second is obtained by adding in quadrature the uncertainties associated with parameters entering both the normalization of the spectral function as well as those from the ‘theoretical’ side of the FESR. The correlation coefficient for the fitted parameters is found to be $c(a_6, a_8) = -0.989$, again corresponding to a highly correlated output.

In like manner to the ALEPH-based determinations of H_1 and H_8 , we have results from OPAL data:

$$\begin{aligned} H_1 &= (-0.4 \pm 3.7 \pm 0.1) \times 10^{-4} \text{ GeV}^6, \\ H_8 &= (0.6 \pm 3.0 \pm 1.0) \times 10^{-4} \text{ GeV}^6. \end{aligned} \quad (25)$$

The errors are treated analogously as in Eq. (23).

Upon adding in quadrature the uncertainties displayed above, we obtain the determinations gathered in Table 1.

3.3. Testing for duality violation

The errors reported above are essentially of an experimental nature. In order to address potential systematic effects due to $R[s_0, w]$ (duality violation), we have repeated the fit procedure in different s_0

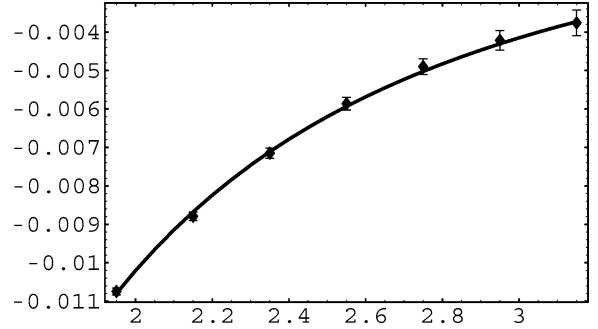


Fig. 3. Variation of f_1 (continuous curve) and J_1 (data) with s_0 (GeV²).

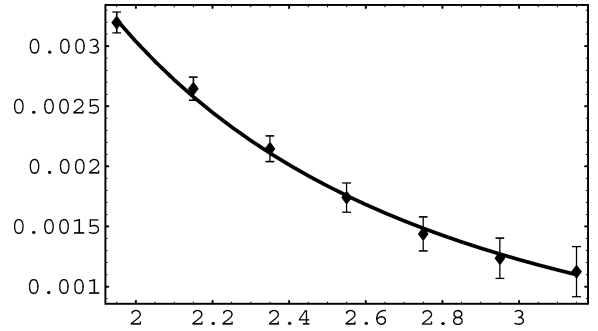


Fig. 4. Variation of f_2 (continuous curve) and J_2 (data) with s_0 (GeV²).

windows (nested sub-windows and nonoverlapping sub-windows). We find that the new values for the fitted parameters are very consistent with each other, thereby confirming that the effect of $R[s_0, w]$ is suppressed in this case. A more explicit and revealing portrait of the FESR machinery is obtained by plotting $J_n(s_0)$ and $f_n(a_6, a_8; s_0)$ as a function of s_0 , as in Figs. 3, 4. In each case, an excellent match of the OPE curve versus data is achieved, showing no sign of duality violation within the present experimental uncertainty.

Given the relatively low values of s_0 used in the analysis, a legitimate worry is that the FESR analysis, despite the excellent match displayed in Figs. 3, 4, might just be extracting the coefficients relevant to the Laurant expansion of the correlator in a sub-asymptotic regime, and not the condensates relevant to the truly asymptotic region. A way to test whether or not we are in such a scenario is to use the condensates extracted in the FESR analysis as input in

a dispersive analysis relevant to the asymptotic regime, and observe the quality of the match there. Such a class of tests is readily possible within explicit models [18, 19] of a given correlator, and shows a very mild pattern of duality violation. Any attempt to perform such tests in the real world is limited by incomplete knowledge of the spectral function. Nonetheless, in our case, with the help of classical sum rules it is possible to construct relevant asymptotic tests, which are described in Ref. [11]. All indications coming from these tests point to negligible duality violation, within the present errors.

4. The electroweak matrix elements

$\langle(\pi\pi)_{I=2}|\mathcal{Q}_{7,8}|K^0\rangle$

In the previous section, we have used the FESR machinery to obtain numerical determinations of OPE coefficients through order $d = 16$. These can be used to obtain the matrix elements $\mathcal{M}_{7,8}$,

$$\mathcal{M}_{7,8} \equiv \frac{\langle(\pi\pi)_{I=2}|\mathcal{Q}_{7,8}|K^0\rangle_{\mu=2\text{ GeV}}^{\overline{\text{MS}}\text{-NDR}}}{1\text{ GeV}^3}. \quad (26)$$

Note in this definition that $\mathcal{M}_{7,8}$ are simply dimensionless numbers. We apply our FESR results via two distinct procedures:

- (1) FESR: insertion of a_6 into Eqs. (5), (8) leads directly to \mathcal{M}_8 , up to a small contribution (at the 5% level) due to $\langle O_1 \rangle$. In the numerical evaluation we use $\langle O_1 \rangle$ from Ref. [4].
- (2) HYBRID: insertion of the FESR-derived quantities $H_{1,8}$ in the sum rules of Eq. (10), together with Eq. (5), leads to both \mathcal{M}_7 and \mathcal{M}_8 . This ‘hybrid’ approach requires as input the integrals

$$\begin{aligned} I_1 &= -(39.7 \pm 3.1) \times 10^{-4} \text{ GeV}^6, \\ I_8 &= -(26.2 \pm 3.0) \times 10^{-4} \text{ GeV}^6, \end{aligned} \quad (27)$$

each evaluated at scale $\mu = 2 \text{ GeV}$ [4].

In Eqs. (8), (10) we use the $n_f = 4$ matching coefficients, appropriate for the renormalization scale $\mu = 2 \text{ GeV}$. Moreover, in relating $\mathcal{M}_{7,8}$ to $\langle O_{1,8} \rangle$ (see Eq. (5)) we use $F_\pi^{(0)} = 87.2 \pm 2.6 \text{ MeV}$. We collect our results in Table 2, and for the sake of completeness

Table 2
Matrix element results

Method	\mathcal{M}_7	\mathcal{M}_8
RWM	0.16 ± 0.10	2.22 ± 0.67
FESR (ALEPH)		1.40 ± 0.28
FESR (OPAL)		1.68 ± 0.32
HYBRID (ALEPH)	0.225 ± 0.046	1.55 ± 0.52
HYBRID (OPAL)	0.210 ± 0.044	1.66 ± 0.46

include our previous sum rule determination (the ‘RWM’ approach of Ref. [4]) as well.

4.1. Comments

The content of Table 2 naturally gives rise to two issues which require further discussion: (i) whether the RWM, FESR and HYBRID results can be combined into a single value, and (ii) whether the ALEPH and OPAL values can be combined into a single value. We consider each in turn.

The FESR method described at length in this Letter utilizes a rather different evaluation procedure from the RWM of Ref. [4]. The HYBRID method is at first glance a consistency check between RWM and FESR which uses the FESR estimations of $H_{1,8}$ (i.e., higher-dimension effects) in evaluating the RWM sum rules at the low scale $\mu = 2 \text{ GeV}$. However, it should be understood that, in the low-scale RWM evaluation of the integrals I_1 and I_8 , about 60% of the full contribution comes from the input values of the chiral constraint integrals, and only about 40% from the integrals over the τ data. Thus the pFESR and hybrid evaluations are to a significant extent independent, and the agreement between the two represents a highly nontrivial mutual check. We note that since the error bars for the FESR results are rather smaller than those for RWM, they would dominate any averaging procedure. As a practical matter, we choose to simply point out that the FESR approach yields our best determination of \mathcal{M}_8 , while the HYBRID approach leads to our best determination of \mathcal{M}_7 , and leave it at that.

Let us hereafter accept the FESR determination as our ‘official’ result. We discuss next the procedure for combining the ALEPH and OPAL evaluations of a_6 and a_8 , beginning with the second uncertainties in Eqs. (22), (24). Since these arise in both ALEPH and

OPAL analyses from the same sources (S_{EW} , B_e , B_π , V_{ud} ; OPE coefficients a_4 and b_6), they are common to both analyses and cannot be reduced by averaging. For definiteness, we adopt for this common uncertainty the midpoint between the ALEPH and OPAL values. As for the first uncertainties in Eqs. (22), (24), they could be treated as ordinary independent errors if the ALEPH and OPAL covariance matrices were fully independent. However, the covariance matrices have a common component since the two experiments share uncertainties due to common normalization input (i.e., OPAL used the 96/97 PDG results for the tau branching ratios and these were dominated by ALEPH measurements). We do not have the detailed knowledge to determine exactly the degree of correlation induced in the output of our ALEPH and OPAL analyses. Therefore, we have performed the averaging assuming a generic correlation coefficient c between the ALEPH and OPAL results. The following combined results correspond to the conservative value $c = 0.5$:

$$a_6 = (-48.1 \pm 5.8 \pm 3.1) \times 10^{-4} \text{ GeV}^6, \quad (28)$$

$$a_8 = (-44.3 \pm 26.6 \pm 12.8) \times 10^{-4} \text{ GeV}^8. \quad (29)$$

Dependence on the correlation parameter c is modest (e.g., for $c = 0$ we obtain $a_6 = (-48.8 \pm 4.7 \pm 3.1) \times 10^{-4} \text{ GeV}^6$ and $a_8 = (-40.9 \pm 21.8 \pm 12.8) \times 10^{-4} \text{ GeV}^8$). Combining the above uncertainties in quadrature yields

$$\begin{aligned} a_6 &= (-48.1 \pm 6.6) \times 10^{-4} \text{ GeV}^6, \\ a_8 &= (-44.3 \pm 29.5) \times 10^{-4} \text{ GeV}^8. \end{aligned} \quad (30)$$

Our final combined numbers for $\mathcal{M}_{7,8}$ in the chiral limit are:

$$\mathcal{M}_7^{\text{chiral}} = 0.22 \pm 0.05, \quad \mathcal{M}_8^{\text{chiral}} = 1.50 \pm 0.27. \quad (31)$$

4.2. Chiral corrections

The above numbers represent our determination of the electroweak penguin matrix elements in the chiral limit, where a data-driven evaluation has been possible. However, to make contact with phenomenology, an estimate of the chiral corrections is mandatory. This issue has been studied by two of us in Ref. [20] within NLO Chiral Perturbation Theory. At this order there are two contributions to the chiral corrections: one

is given by the chiral loops and comes with no uncertainty, while the other is due to local couplings in the effective theory, not known accurately at present. A conservative estimate of these couplings, based on naive dimensional analysis (and supported by an explicit calculation in leading $1/N_c$ [21]), gives

$$\mathcal{M}_{7,8}^{\text{physical}} = \mathcal{M}_{7,8}^{\text{chiral}} \times F_\chi, \quad (32)$$

where F_χ represents the dispersive and absorptive corrections (generated at NLO) to the matrix elements [20],

$$F_\chi = (0.7 \pm 0.2) - i0.21. \quad (33)$$

That the determination of F_χ is less firm than that of $\mathcal{M}_{7,8}^{\text{chiral}}$ is reflected in its relatively larger uncertainty. Adopting the result of Eq. (33), we are led to quote

$$\begin{aligned} |\mathcal{M}_7^{\text{physical}}| &= 0.16 \pm 0.035_{\chi\text{-lim}} \pm 0.044_{\chi\text{-corr}} \\ &= 0.16 \pm 0.06, \end{aligned} \quad (34)$$

$$\begin{aligned} |\mathcal{M}_8^{\text{physical}}| &= 1.10 \pm 0.20_{\chi\text{-lim}} \pm 0.30_{\chi\text{-corr}} \\ &= 1.10 \pm 0.36. \end{aligned} \quad (35)$$

We shall use $\mathcal{M}_8^{\text{physical}}$ to estimate the electroweak penguin contribution to ϵ'/ϵ .

4.3. Comparison with other analyses

We observe that other analyses of the V–A correlator exist in the literature [22–25] which give generally different values of the OPE coefficients from those found here (especially for the a_d with $d > 6$). The relation between our analysis and these others will be discussed in a companion paper [11].

Here we focus on the comparison with other determinations of $\mathcal{M}_{7,8}$ in the chiral limit, based on alternate nonperturbative methods. The analytic methods of Refs. [24,26,27] work directly in the chiral limit, while the lattice results refer to chiral limit extrapolations, explicitly reported in Refs. [28–30]. When necessary, we have converted the lattice results to the $\overline{\text{MS}}$ -NDR scheme at $\mu = 2 \text{ GeV}$. Moreover, lattice results are obtained in the quenched approximation and the quoted error is only statistical. Finally, let us recall that other determinations of electroweak matrix elements can be found in Ref. [31].

Our value for \mathcal{M}_8 is slightly higher than the lattice determinations. However, the agreement is

Table 3

	\mathcal{M}_7	\mathcal{M}_8
This work	0.22 ± 0.05	1.50 ± 0.27
Bijnens et al. [26]	0.24 ± 0.03	1.2 ± 0.7
Knecht et al. [27]	0.11 ± 0.03	2.34 ± 0.73
Narison [24]	0.21 ± 0.05	1.4 ± 0.35
RBC (DWF) [28]	0.28 ± 0.04	1.1 ± 0.2
CP-PACS (DWF) [29]	0.24 ± 0.03	1.0 ± 0.2
SPQcdR (Wilson) [30]	0.24 ± 0.02	1.05 ± 0.10
Vacuum Saturation	0.32	0.94

better than previous work had indicated. The present lattice results are larger than earlier lattice estimates while our new result is about one standard deviation below our previous central value. Given that the lattice results are in the quenched limit, the present level of agreement is satisfactory. Lattice estimates of \mathcal{M}_7 are also in agreement with our results. Finally, the results of Refs. [24,26,27] also seem in reasonable agreement with ours, with the possible exception of the smaller \mathcal{M}_7 result of Ref. [27].

5. Conclusion

This Letter has described an improved chiral determination of the electroweak penguin contribution to ϵ'/ϵ . Let us summarize the nature of the improvement over our previous result. Recall that our determinations are not calculations in the usual sense of constructing an approximation to QCD which is then used to calculate the operator matrix element. Rather, our methods start from the observation that the matrix elements of the electroweak penguin operators $\mathcal{Q}_{7,8}$ become related in the chiral limit to the vacuum matrix elements of two other operators, and that these vacuum matrix elements can be determined from existing experimental data. Our previous determinations and those of the present Letter are based on different approaches to extracting these vacuum matrix elements. Much of our work has been devoted to minimizing the impact on our final uncertainties of both the absence of spectral data above $s = m_\tau^2$ and the presence of large experimental errors near the upper end of the kinematically accessible range. A detailed understanding of these uncertainties has also been obtained.

Our earlier chiral determination of $[\epsilon'/\epsilon]_{\text{EWP}}$ (cf. Eq. (4)) was based on the use of other rigorous

chiral sum rules in order to minimize the effect where the data were poor or nonexistent. This is a very direct approach, and we found that it carried a 32% uncertainty. The error bar was partially due to the residual experimental uncertainty from the tau decay data. However the error bar also had a large component due to uncertainties in the inputs to the other chiral sum rules which were used as constraints, the largest of which involved the pion's electromagnetic mass difference in the chiral limit. For example, at $\mu = 4$ GeV (where it is safe to neglect higher-dimensional contributions) the result was a determination of \mathcal{M}_8 with 32% uncertainty. Roughly 80% of the error on the dispersive integral $I_8(4 \text{ GeV})$ is due to uncertainties in the inputs to the chiral sum rule constraints, the dominant contribution being the above-mentioned uncertainty in the chiral limit value of the pion electromagnetic mass splitting.

The present evaluation, based on the FESR method, does not use the chiral sum rules and hence does not share the same uncertainties. Rather, the FESR error bars arise primarily from uncertainties in the tau decay data. We use doubly pinched weights in the FESR integrals both to minimize the influence of these data uncertainties and also to suppress OPE contributions from the vicinity of the timelike real axis. Presumably, the latter effect serves to improve the reliability of the OPE representation for $\Delta\Pi$. To perform a highly nontrivial check of this presumption, we extract each OPE coefficient a_d with more than one weight.⁵ In all cases, excellent consistency is found. An instructive demonstration is provided by Figs. 3, 4, which involve the determination of a_6 and a_8 using the weights w_1 and w_2 . By design, w_1 and w_2 have very different profiles and thus probe the spectral function in very different ways. The spectral integrals for both the $w_{1,2}$ -weighted FESR's turn out to scale very closely with $1/s_0^2$ (each case implying that the $d = 8$ contribution is small) and the consistency between the a_6 values thus extracted turns out to be excellent. Our procedure has passed a number of additional tests, as will be described elsewhere [11]. Therefore, once one

⁵ The motivation behind this strategy is that, if using the OPE were indeed dangerous (e.g., the integrated OPE therefore gives a poor representation of the data), then one should expose this flaw by using both weights simultaneously.

makes sure that the systematics of the FESR approach are under control, the FESR analysis leads to a more precise determination of \mathcal{M}_8 , because it exploits in an optimal manner the existing database and (unlike the RWM) does not rely on other input.

When we translate the measurement of the OPE coefficient into the electroweak penguin contribution to ϵ' , we find

$$[\epsilon'/\epsilon]_{\text{EWP},\chi\text{-lim}} = (-15.0 \pm 2.7) \times 10^{-4}, \quad (36)$$

in the chiral limit. This is consistent with our previous determination, but has about half (at 18%) the uncertainty. When we include the chiral corrections as described in Section 4.2, we find

$$[\epsilon'/\epsilon]_{\text{EWP,phys}} = (-11.0 \pm 3.6) \times 10^{-4}. \quad (37)$$

The larger error (about 32%) cited for the ‘physical’ result reflects uncertainties in our estimate for the chiral corrections. We note that for the Standard Model to successfully describe ϵ' will require a rather large and positive effect from the standard gluonic penguin operator \mathcal{Q}_6 . Our approach does not provide a determination of this matrix element.

In addition to describing the electroweak penguin contribution to ϵ' , our work is useful in other contexts. We have a firm determination of the \mathcal{Q}_8 nonleptonic matrix element in the chiral limit as well as that for \mathcal{Q}_7 , and there are few such examples that are experimentally known. The results are useful for comparison with models, some of which are included in the comparisons Table 3 in Section 4.3, or for the testing of lattice methods. Our methods may also be adapted rather directly to lattice techniques, because the correlation functions that we work with are readily measured with lattice data. We have started work to make this connection firmer, and will report on the results in the future.

Acknowledgements

The work of J.D. and E.G. was supported in part by the National Science Foundation under Grant PHY-9801875. The work of V.C. was supported in part by MCYT, Spain (Grant No. FPA-2001-3031) and by ERDF funds from the European Commission. K.M. would like to acknowledge the ongoing support of the Natural Sciences and Engineering Research Council

of Canada. We are happy to acknowledge useful input from S. Menke, M. Papinutto, S. Peris, A. Pich, J. Prades and M. Roney.

References

- [1] Y. Nir, Talk given at 31st Intl. Conf. on High Energy Physics, Amsterdam, 24–31 July 2002, hep-ph/0208080; NA48 Collaboration, J.R. Batley, et al., Phys. Lett. B 544 (2002) 97, hep-ex/0208009; KTeV Collaboration, A. Alavi-Harati, et al., hep-ex/0208007.
- [2] E.g., see, A.J. Buras, hep-ph/9806471; A.J. Buras, hep-ph/9901409.
- [3] M. Ciuchini, E. Franco, G. Martinelli, L. Reina, hep-ph/9503277.
- [4] V. Cirigliano, J.F. Donoghue, E. Golowich, K. Maltman, Phys. Lett. B 522 (2001) 245, hep-ph/0109113.
- [5] S. Weinberg, Phys. Rev. Lett. 18 (1967) 507.
- [6] T. Das, G.S. Guralnik, V.S. Mathur, F.E. Low, J.E. Young, Phys. Rev. Lett. 18 (1967) 759.
- [7] ALEPH Collaboration, R. Barate, et al., Z. Phys. C 76 (1997) 15; ALEPH Collaboration, R. Barate, et al., Eur. Phys. J. C 4 (1998) 409.
- [8] OPAL Collaboration, K. Ackerstaff, et al., Eur. Phys. J. C 7 (1999) 571, hep-ex/9808019.
- [9] G. Amoros, J. Bijnens, P. Talavera, Nucl. Phys. B 602 (2001) 87, hep-ph/0101127.
- [10] Aspects of the work described here and some preliminary results are given in V. Cirigliano, talk given at Intl. Conf. on Quantum Chromodynamics, Montpellier, France, July 2–9 2002, hep-ph/0209332; E. Golowich, Talk given at 31st Intl. Conf. on High Energy Physics, Amsterdam, 24–31 July 2002; K. Maltman, Talk at the 7th Intl. Workshop on Tau Lepton Physics, Santa Cruz, CA, USA, 10–14 September 2002, hep-ph/0209091.
- [11] V. Cirigliano, J.F. Donoghue, E. Golowich, K. Maltman, in preparation.
- [12] J.F. Donoghue, E. Golowich, Phys. Lett. B 478 (2000) 172, hep-ph/9911309.
- [13] A.J. Buras, M. Jamin, M.E. Lautenbacher, P.H. Weisz, Nucl. Phys. B 400 (1993) 37, hep-ph/9211304.
- [14] M. Ciuchini, E. Franco, G. Martinelli, L. Reina, Nucl. Phys. B 415 (1994) 403, hep-ph/9304257.
- [15] E.C. Poggio, H.R. Quinn, S. Weinberg, Phys. Rev. D 13 (1976) 1958.
- [16] K. Maltman, Phys. Lett. B 440 (1998) 367, hep-ph/9901239.
- [17] G. D’Agostini, On the use of the covariance matrix to fit correlated data, DESY preprint 93-175, December 1993.
- [18] M. Golterman, S. Peris, JHEP 0101 (2001) 028, hep-ph/0101098.
- [19] S.R. Beane, Phys. Rev. D 64 (2001) 116010, hep-ph/0106022.
- [20] V. Cirigliano, E. Golowich, Phys. Lett. B 475 (2000) 351, hep-ph/9912513;

- V. Cirigliano, E. Golowich, *Phys. Rev. D* 65 (2002) 054014, hep-ph/0109265.
- [21] E. Pallante, A. Pich, I. Scimemi, *Nucl. Phys. B* 617 (2001) 441, hep-ph/0105011.
- [22] B.L. Ioffe, K.N. Zyablyuk, *Nucl. Phys. A* 687 (2001) 437, hep-ph/0010089.
- [23] M. Davier, L. Girlanda, A. Hocker, J. Stern, *Phys. Rev. D* 58 (1998) 096014, hep-ph/9802447.
- [24] S. Narison, *Nucl. Phys. B* 593 (2001) 3, hep-ph/0004247.
- [25] S. Peris, B. Phily, E. de Rafael, *Phys. Rev. Lett.* 86 (2001) 14, hep-ph/0007338.
- [26] J. Bijnens, E. Gamiz, J. Prades, *JHEP* 0110 (2001) 009, hep-ph/0108240.
- [27] M. Knecht, in: *Proc. Intl. Conf. on High Energy Physics, HEP2001/226*;
- An earlier version appears in M. Knecht, S. Peris, E. de Rafael, *Phys. Lett. B* 508 (2001) 117, hep-ph/0102017.
- [28] RBC Collaboration, T. Blum, et al., hep-lat/0110075.
- [29] CP-PACS Collaboration, J.I. Noaki, et al., hep-lat/0108013.
- [30] SPQCDR Collaboration, D. Becirevic, et al., hep-lat/0209136.
- [31] A. Donini, V. Gimenez, L. Giusti, G. Martinelli, *Phys. Lett. B* 470 (1999) 233, hep-lat/9910017; T. Bhattacharya, et al., *Nucl. Phys. (Proc. Suppl.)* 106 (2002) 311, hep-lat/0111004; T. Hambye, G.O. Kohler, E.A. Paschos, P.H. Soldan, W.A. Bardeen, *Phys. Rev. D* 58 (1998) 014017, hep-ph/9802300; S. Bertolini, J.O. Eeg, M. Fabbrihesi, E.I. Lashin, *Nucl. Phys. B* 514 (1998) 93, hep-ph/9706260.